Bioorganic & Medicinal Chemistry Letters 19 (2009) 2630–2633

Contents lists available at ScienceDirect

Bioorganic & Medicinal Chemistry Letters

journal homepage: www.elsevier.com/locate/bmcl

Computer-aided rational molecular design of argifin-derivatives with increased inhibitory activity against chitinase B from *Serratia marcescens*

Hiroaki Gouda [a], Toshiaki Sunazuka [b], Kanami Iguchi [b], Akihiro Sugawara [b], Tomoyasu Hirose [b], Yoshihiko Noguchi [b], Yoshifumi Saito [b], Yuichi Yanai [a], Tsuyoshi Yamamoto [b], Takeshi Watanabe [c], Kazuro Shiomi [b], Satoshi Ōmura [b,*], Shuichi Hirono [a,*]

[a] *School of Pharmacy, Kitasato University, 5-9-1 Shirokane, Minato-ku, Tokyo 108-8641, Japan*
[b] *Kitasato Institute for Life Sciences, Graduate School of Infection Control Science, School of Pharmaceutical Sciences, Kitasato University, 5-9-1 Shirokane, Minato-ku, Tokyo 108-8641, Japan*
[c] *Department of Applied Biological Chemistry, Faculty of Agriculture, Niigata University, 8050 Ikarashi-2, Niigata 950-2181, Japan*

ARTICLE INFO

Article history:
Received 19 February 2009
Revised 2 April 2009
Accepted 3 April 2009
Available online 9 April 2009

Keywords:
In silico drug design
Molecular dynamics
Docking
Binding free energy

ABSTRACT

Argifin, a novel pentapeptide chitinase inhibitor isolated from *Gliocladium* fungal culture, is a promising candidate for the development of new fungicides, insecticides, and anti-asthma medications. In this study, we undertook rational molecular design of argifin-derivatives and tested them against chitinase B from *Serratia marcescens* (*Sm*ChiB). The work involved molecular dynamics simulation with explicit water molecules, the molecular docking calculation, and free-energy analysis using the molecular mechanics Poisson–Boltzmann surface area method. The custom-designed derivatives were synthesized via effective solid phase synthesis, developed recently in our laboratory, and their inhibitory activities were measured against *Sm*ChiB. Finally, we identified and obtained a derivative which exhibited 28-fold more inhibition than argifin itself, a compound in which the D-Ala(5) of argifin was replaced with D-Leu and the 4-benzylpiperdine was attached to L-Asp(4).

© 2009 Elsevier Ltd. All rights reserved.

Family 18 chitinases hydrolyze β-(1,4)-linked *N*-acetylglucosamine (Chitin), which is one of the most abundant polysaccharides in nature. These enzymes are present in a wide range of organisms including bacteria, fungi, insects, mammals and humans.[1–5] As chitin is a major structural component of fungi and insects, family 18 chitinases play important physiological roles in these organisms.[2,3,6,7] It has been also reported that mammalian acidic chitinase is implicated in triggering asthma.[8] Therefore, chitinase inhibitors have attractive potential to function as fungicides, insecticides and anti-asthma medications.[9–11] Nevertheless, no practical use for chitinase inhibitors has been developed to date. During screening for chitinase inhibitors in our laboratory, a novel cyclic pentapeptide Argifin (**1**) was isolated from the culture broth of *Gliocladium* sp. FTD-0668 (Fig. 1).[12] It seems to be a good candidate for the development of novel drugs, due to its potent inhibitory activity against chitinases[12,13] and the recent establishment of total synthesis strategies, independently established by Eggleston et al. and our groups.[14,15] The three-dimensional (3D) structure of **1**, in complex with chitinase B from *Serratia marcescens* (*Sm*ChiB), was resolved by X-ray crystallography.[16] Argifin inhibits *Sm*ChiB with a half-maximal inhibitory concentration (IC_{50}) value of 6.4 μM.[15] These factors and observations stimulated us to try and design argifin-derivatives with more potent inhibitory activity. Therefore, we describe here the rational molecular design strategy we devised for argifin-derivatives, which consists of molecular dynamics (MD) simulation, the molecular docking calculation, and the free-energy analysis (using the molecular mechanics Poisson–Boltzmann surface area (MM-PBSA) method).[17]

We had already performed the MD simulation with explicit water molecules for 1700 ps length using the crystal structure of *Sm*ChiB–argifin complex (PDB:1H0I) as an initial coordinate, in order to obtain the ensemble of its solution structures.[18] Consequently, we first used a total of 200 snapshots derived from the MD trajectory to perform the 2D root-mean-square deviation (RMSD) analysis on the binding site, which included argifin and 26 residues from *Sm*ChiB, by *ptraj* module of AMBER 8.[19] This allowed us to group a number of snapshots into several different kinds of conformations. As a result, we obtained two representative solution structures of the argifin–*Sm*ChiB complex, that is, snapshots at 890 and 1505 ps, (which are referred to as S890 and S1505, respectively (see Supplementary Figs. 1 and 2)). Both S890 and S1505 used the L-Arg(1) and L-Asp(3) of argifin to form a total of six hydrogen bonds with W97, D142, E144, Y214, and D215 of *Sm*ChiB, including five identified in the crystal structure. The other interaction feature is an aromatic stacking interaction

* Corresponding authors. Tel.: +81 3 5791 6101; fax: +81 3 3444 8360 (S.O.); tel.: +81 3 3443 7780; fax: +81 3 3440 5246 (S.H.).
E-mail addresses: omura-s@kitasato.or.jp (S. Ōmura), hironos@pharm.kitasato-u.ac.jp (S. Hirono).

0960-894X/$ - see front matter © 2009 Elsevier Ltd. All rights reserved.
doi:10.1016/j.bmcl.2009.04.013

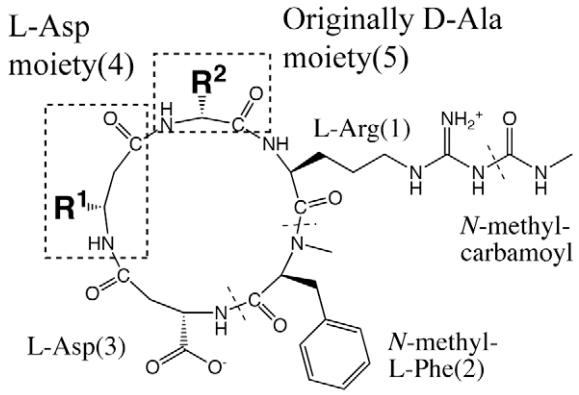

Derivatives	R^1 in L-Asp moiety(4)	D-amino acids(5) (includin g R^2)
Argifin (**1**)	-COOH	D-Ala
2	-CO(4-Benzylpiperdinyl)	D-Ala
3	-COOH	D-Val
4	-COOH	D-Leu
5	-COOH	D-Met
6	-COOH	D-Phe
7	-COOH	D-Trp
8	-CO(4-Benzylpiperdinyl)	D-Leu

Figure 1. Chemical structures of argifin (**1**) and artificial derivatives **2**–**8**.

between the *N*-methyl-L-Phe(2) of argifin and W97, F191 and W220 of *Sm*ChiB. S890 and S1505 mainly differ in the salt-bridge structure formed by D316, D336, and R338 of *Sm*ChiB, which is close to the L-Asp(4) of argifin. Thus, the MD simulation allows us to consider the dynamic behavior of bio-molecules in the rational molecular design by providing several different kinds of conformations.

Two representative structures, that is, S890 and S1505, were used to obtain guides for designing argifin derivatives. As described above, the L-Arg(1), *N*-methyl-L-Phe(2) and L-Asp(3) of argifin appear to be essential for binding. In addition, the available space around *N*-methyl-L-Phe(2) seems to be too small to accommodate a more bulky residue such as Trp. Therefore, attention shifted to two other residues of argifin, that is, L-Asp(4) and D-Ala(5). As shown in Figure 2A (see also Supplementary Fig. 2), three acidic residues of *Sm*ChiB, that is, E315, D316, and D336, were located very close to L-Asp(4) of argifin, suggesting the presence of unfavorable electrostatic interaction. Therefore, we got an idea, the modification of carboxyl group of L-Asp(4) to neutral or positive groups. However, due to the prospect of synthetic accessibility, we could envisage only one derivative, that is, 2, in which the 4-benzylpiperdine group replaces a carboxylate oxygen of L-Asp(4) (Fig. 1). We speculated that the introduction of this group might not cause severe crash with *Sm*ChiB, because L-Asp(4) of argifin was exposed to solvent in both S890 and S1505. Further, we found an interesting deep groove close to L-Asp(4) of argifin in S890, which is formed by D316, P317, Y318, P319, K335, D336, and R338 of *Sm*ChiB (Fig. 2A). We expected that the 4-benzylpiperdinyl group of the derivative **2** might form additional interactions within this groove. We also found a wide space to accommodate more bulky side chains around D-Ala(5) of argifin in both S890 and S1505 (Fig. 2A). Subsequently, we also designed five derivatives (**3–7**) in which D-Ala(5) was mutated to D-Val, D-Leu, D-Met, D-Phe, and D-Trp (Fig. 1), in order to make additional contacts with F12, F51, Y98, and W403 of *Sm*ChiB. The chemical structures of derivatives are depicted in Supplementary Fig. 3.

The interaction mode of each derivative with *Sm*ChiB was predicted as follows, that is, the conformational analysis of the ring structure was first performed using the CAMDAS 2.1 (Conformational Analyzer with Molecular Dynamics and Sampling) programme,[20] because the flexibility of the ring structure is not considered in the general docking programme, so we needed to prepare different ring conformations prior to the docking calculation. Next, the molecular docking calculation of conformers obtained by CAMDAS was performed against the binding sites of S890 and S1505 with Glide version 4.0 (SP mode),[21] and the generated poses were ranked according to Glidescore. On the top 100 poses, the MM-PBSA method was applied to estimate the free energies of their complex structures ($G_{complex}$s). Finally, we selected a pose with the lowest $G_{complex}$ as the interaction model. The details of our pro-

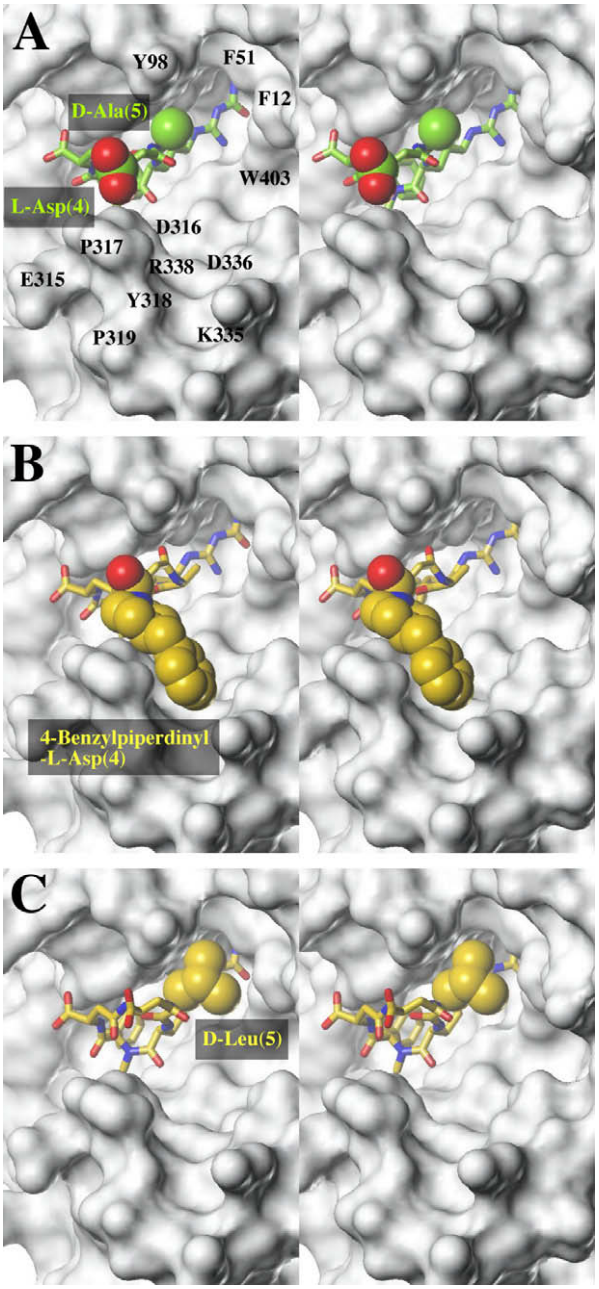

Figure 2. Stereoview of interaction of argifin in S890 (A), and those of derivatives **2** (B) and **4** (C) obtained by our procedure. L-Asp(4) and D-Ala(5) of argifin, 4-benzylpiperdinyl-L-Asp(4) of derivative **2**, and D-Leu(5) of derivative **4**, are shown in space-filling display.

Table 1
ΔG_{bind}, $\Delta\Delta G_{bind}$ and LE index estimated by the MM-PBSA method, overall yields for solid phase synthesis, and inhibitory activities against *Sm*ChiB for argifin (**1**) and derivatives **2**–**8**

Derivatives	ΔG_{bind}[a] (kcal/mol)	$\Delta\Delta G_{bind}$[a] (kcal/mol)	LE index	Yields[b] (%)	IC_{50} (μM) against *Sm*ChiB[c]
Argifin (**1**)	−45.81	0.00	−6.61	13	6.4 ± 1.0
2	−55.54	−9.73	−7.17	24	1.3 ± 0.11
3	−46.61	−0.80	−6.59	7.4	6.1 ± 0.37
4	−49.33	−3.52	−6.91	8.6	1.9 ± 0.27
5	−47.89	−2.08	−6.71	10	10.0 ± 0.59
6	−49.31	−3.50	−6.71	7.9	9.9 ± 1.2
7	−53.72	−7.91	−7.12	6.3	4.5 ± ± 0.55
8	−57.34	−11.53	−7.22	37	0.23 ± 0.054

[a] Solute entropy term is not included (see Supplementary data).
[b] Isolation yields by HPLC purification after cleaving from 2-chlorotrityl resin.
[c] See Ref. 15 for IC_{50} measurement.

cedure are provided in Supplementary data. We should emphasize that our procedure could accurately reproduce the interaction mode of argifin with *Sm*ChiB (Supplementary Fig. 5). All derivatives preferred the binding sites of S890, and retained the interactions between argifin and *Sm*ChiB observed in S890. As expected, the interaction model of **2** located its 4-benzylpiperdinyl group in the target groove to make an additional van der Waals interaction with *Sm*ChiB (Fig. 2B). The calculations also predicted that all side-chains of D-Val(5), D-Leu(5), D-Met(5), D-Phe(5), and D-Trp(5) of **3**–**7** could occupy the available space around D-Ala(5) in the argifin–*Sm*ChiB complex. As an example, the interaction model of **4** is shown in Figure 2C. Other models are included in Supplementary Fig. 6. In our previous study,[18] we reported work on derivatives **3**, **4**, **6**, and **7** covering a very simple substitution modeling method, in which D-Ala(5) of argifin in the complex structure was just replaced to D-Val, D-Leu, D-Phe, and D-Trp, and the orientation of their side-chains were explored to minimize the crash with *Sm*ChiB. The orientations of D-Val(5), D-Leu(5), and D-Phe(5) of derivatives **3**, **4**, and **6**, respectively, were found to be almost the same between the docking calculation and the simple substitution modeling, but the orientation of D-Trp(5) of **7** was different between the two methods. These results suggest that the rigorous molecular docking calculation is indispensable for derivatives with the introduction of large side-chains, since it can translate and rotate the whole of a molecule to locate them in a more suitable site.

The binding affinity (ΔG_{bind}) of each derivative was approximated by applying the single-point MM-PBSA calculation (see Supplementary data). The relative binding affinity ($\Delta\Delta G_{bind}$) was estimated using the ΔG_{bind} value of argifin in S890 as a reference. The results are summarized in Table 1. All derivatives showed greater ΔG_{bind} values than argifin, indicating that they might have better binding affinities. The derivative **2** showed much greater electrostatic interaction with *Sm*ChiB than argifin as expected, but the gain was completely lost by less favorable contribution of electrostatic component to solvation (see Supplementary Table 2). Therefore, the total electrostatic component of the binding free energy of the derivative **2** was predicted to be less favorable than that of argifin. However, more favorable van der Waals contribution led to a better ΔG_{bind} value of the derivative **2**. These results indicated that the ligand optimization in the electrostatic point of view might be a delicate issue, as we need to consider the electrostatic component to solvation as well as the electrostatic interaction energy. On the other hand, the source of better ΔG_{bind} values for the derivative **3**–**7** was mainly derived from more favorable van der Waals interactions as expected. We also obtained a kind of 'ligand efficiency index' for each derivative by a similar manner to that of Huang et al.,[22] which was calculated by dividing a value of ΔG_{bind} by a root of the number of heavy atoms, in order to prioritize the derivatives. The LE indices suggested that only three derivatives, namely **2**, **4**, and **7**, showed much better ligand effi-

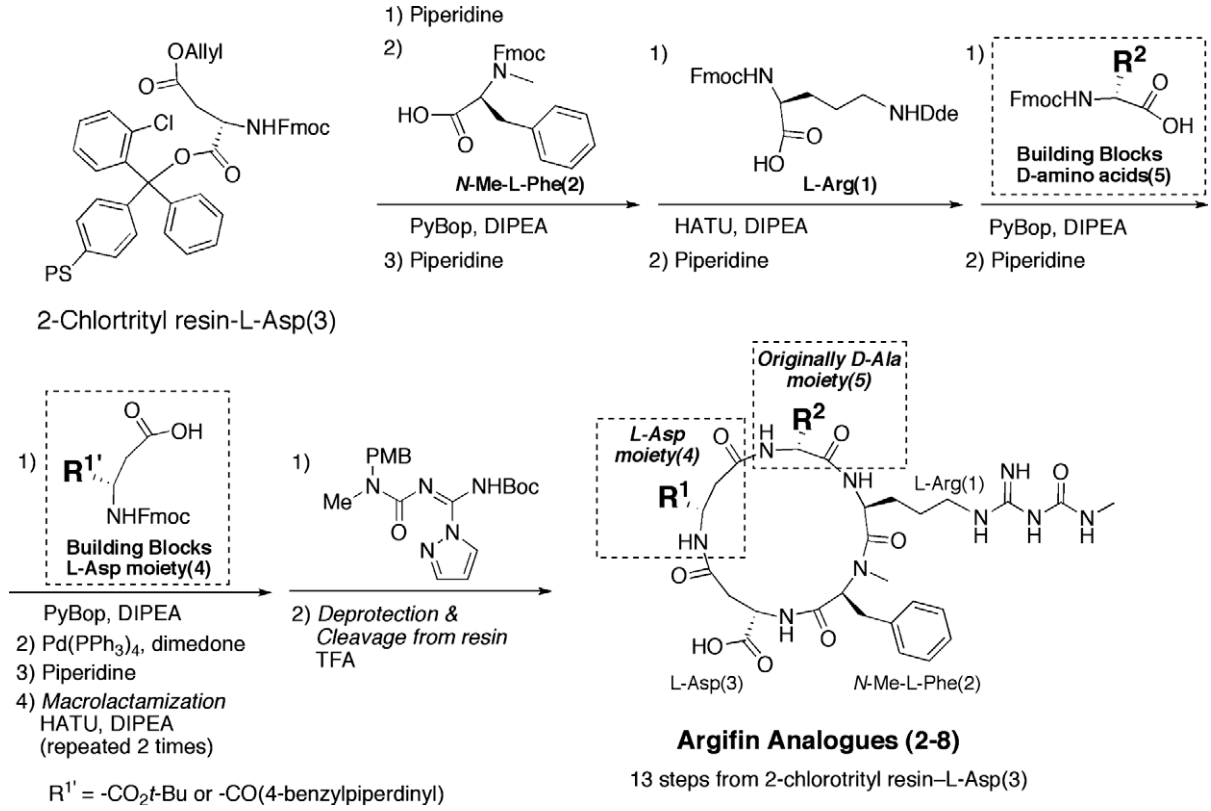

Scheme 1. Synthesis of our argifin library.

ciency than argifin. Therefore, we expected that these three derivatives were most likely to have better binding affinities, that is, possess more potent inhibitory activity, than argifin.

We have previously developed an efficient solid-phase, total synthesis of argifin, involving macrolactonization on resin, as well as construction of the N^{ω}-methylcarbamoyl group, with single HPLC purification.[15] Initially, we synthesized the above 6-derivative library (**2**–**7**) based on the natural argifin scaffold, according to our synthetic strategy using building blocks of D-amino acid(5) [D-Val, D-Leu, D-Met, D-Phe and D-Trp] and L-Asp moiety(4) [$R^{1'}$ = –CO_2*t*-Bu and –CO(4-benzylpiperdinyl)], as summarized in Scheme 1. These cyclic derivatives were purified by preparative reversed phase HPLC after cleaving from 2-chlorotrityl resin.[23]

For the determination of IC_{50} values against *Sm*ChiB, the derivatives were compared in a competition assay with 4-methylumberiferyldiacetyl-chitobiose.[15,24,25] The results are shown in Table 1. As expected, derivatives **2**, **4** and **7** were found to possess higher inhibitory activities against *Sm*ChiB with IC_{50} values of 1.3, 1.9, and 4.5 μM, respectively, than argifin (6.4 μM). These results indicated that our design strategy is very useful for obtaining more potent derivatives. Further, we hypothesized that a hybrid derivative (**8**), effectively a combination of **2** and **4**, may exhibit enhanced inhibitory potency. The docking calculation also suggested this possibility (Table 1 and Supplementary Fig. 6). Hence, we synthesized **8** and measured its inhibitory activity. As expected, **8** was found to be most potent inhibitor against *Sm*ChiB, with an IC_{50} value of 0.23 μM, which was about a 28-fold increase over that of argifin.

In this study, we successfully performed the rational molecular design of argifin-derivatives, and obtained a derivative (**8**) which showed about 28 times more potent inhibitory activity than argifin itself. We believe that our strategy could be applied to a variety of chitinases derived from fungi, insects, and humans and will prove useful for the development of novel fungicides, insecticides and anti-asthma medications based on argifin.

Acknowledgments

This work was supported, in part, by Grant-in-Aid for Scientific Research (C) of the Japan Society for the Promotion of Science [KAKENHI 19590043 (H.G.) and KAKENHI 18590015 (T.S.)], the Takeda Science Foundation, the Mochida Memorial Foundation for Medical and Pharmaceutical Research the Research Fellowships of the Japan Society for the Promotion of Science for Young Scientists (A.S.), and by the Kitasato University Research Grant for Young Researchers (H.G.).

Supplementary data

Supplementary data associated with this article can be found, in the online version, at doi:10.1016/j.bmcl.2009.04.013.

References and notes

1. Brurberg, M. B.; Nes, I. F.; Eijsink, V. G. H. *Microbiology* **1996**, *142*, 1581.
2. Kuranda, M. J.; Robbins, P. W. *J. Biol. Chem.* **1991**, *266*, 19758.
3. Merzendorfer, H.; Zimoch, L. *J. Exp. Biol.* **2003**, *206*, 4393.
4. Renkema, G. H.; Boot, R. G.; Muijsers, A. O.; Donker-Koopman, W. E.; Aerts, J. M. F. G. *J. Biol. Chem.* **1995**, *270*, 2198.
5. Boot, R. G.; Blommaart, E. F. C.; Swart, E.; Ghauharali-van der Vlugt, K.; Bijl, N.; Moe, C.; Place, A.; Aerts, J. M. F. G. *J. Biol. Chem.* **2001**, *276*, 6770.
6. Takaya, N.; Yamazaki, D.; Horiuchi, H.; Ohta, A.; Takagi, M. *Biosci. Biotechnol. Biochem.* **1998**, *62*, 60.
7. Cohen, E. *Arch. Insect. Biochem. Physiol.* **1993**, *22*, 245.
8. Zhu, Z.; Zheng, T.; Homer, R. J.; Kim, Y. K.; Chen, N. Y.; Cohn, L.; Hamid, Q.; Elias, J. A. *Science* **2004**, *304*, 1678.
9. Kawada, M.; Hachiya, Y.; Arihiro, A.; Mizoguchi, E. *Keio J. Med.* **2007**, *56*, 21.
10. Shiomi, K.; Arai, N.; Iwai, Y.; Turberg, A.; Kölbl, H.; Ōmura, S. *Tetrahedron Lett.* **2000**, *41*, 2141.
11. Izumida, H.; Nishijima, M.; Takadera, T.; Nomoto, A. M.; Sano, H. *J. Antibiot.* **1996**, *49*, 829.
12. Ōmura, S.; Arai, N.; Yamaguchi, Y.; Masuma, R.; Iwai, Y.; Namikoshi, M.; Turberg, A.; Kölbl, H.; Shiomi, K. *J. Antibiot.* **2000**, *53*, 603.
13. Arai, N.; Shiomi, K.; Yamaguchi, Y.; Masuma, R.; Iwai, Y.; Turberg, A.; Kölbl, H.; Ōmura, S. *Chem. Pharm. Bull.* **2000**, *48*, 1442.
14. Dixon, M. J.; Andersen, O. A.; van Aalten, D. M.; Eggleston, I. M. *Bioorg. Med. Chem. Lett.* **2005**, *15*, 4717.
15. Sunazuka, T.; Sugawara, A.; Iguchi, K.; Hirose, T.; Nagai, K.; Noguchi, Y.; Saito, Y.; Yamamoto, T.; Ui, H.; Gouda, H.; Shiomi, K.; Watanabe, T.; Ōmura, S. *Bioorg. Med. Chem.* **2009**, *17*, 2751.
16. Houston, D. R.; Shiomi, K.; Arai, N.; Ōmura, S.; Peter, M. G.; Turberg, A.; Synstad, B.; Eijsink, V. G. H.; van Aalten, D. M. F. *Proc. Natl. Acad. Sci. U.S.A.* **2002**, *99*, 9127.
17. Kollman, P. A.; Massova, I.; Reyes, C.; Kuhn, B.; Huo, S.; Chong, L.; Lee, M.; Lee, T.; Duan, Y.; Wang, W.; Donini, O.; Cieplak, P.; Srinivasan, J.; Case, D. A.; Cheatham, T. E., III *Acc. Chem. Res.* **2000**, *33*, 889.
18. Gouda, H.; Yanai, Y.; Sugawara, A.; Sunazuka, T.; Ōmura, S.; Hirono, S. *Bioorg. Med. Chem.* **2008**, *16*, 3565.
19. Case, D. A.; Darden, T. A.; Cheatham III, T. E.; Simmerling, C. L.; Wang, J.; Duke, R. E.; Luo, R.; Merz, K. M.; Wang, B.; Pearlman, D. A.; Crowley, M.; Brozell, S.; Tsui, V.; Gohlke, H.; Mongan, J.; Hornak, V.; Cui, G. Beroza, P.; Schafmeister, C.; Caldwell, J. W.; Ross, W. S.; Kollman, P. A. AMBER8; University of California: San Francisco, 2004.
20. Tsujishita, H.; Hirono, S. *J. Comput. Aided Mol. Des.* **1997**, *11*, 305.
21. GLIDE, *version* 4.0; Schrödinger, LLC: New York, 2007.
22. Huang, N.; Nagarsekar, A.; Xia, G.; Hayashi, J.; MacKerell, A. D., Jr. *J. Med. Chem.* **2004**, *47*, 3502.
23. Dry DMF, CH_3CN, TFA and CH_2Cl_2 were purchased from Kanto Chemical Co. Preparative HPLC (UV at 210 nm, Senshu Pak. PEGASIL ODS, 20ø × 250 mm with isocratic conditions between 13% and 35% acetonitrile containing 0.05% TFA/aqueous at a flow rate of 8.0 mL/min). ^{1}H and ^{13}C NMR spectra were measured on Varian XL-400 (400 MHz and 100 MHz) with CD_3OD or D_2O. All infrared spectra were measured on a Horiba FT-210 spectrometer. High- and low-resolution mass spectra were measured on a JEOL JMS-DX300 and JEOL JMS-AX505 HA spectrometer. The data for an analogue (**8**) is included as an example: a light brown amorphous; IR (KBr) ν cm^{-1}: 3300, 3081, 3030, 1674, 1558, 1496, 1464; $[\alpha]_D^{24}$ = −40.8 (*c* 1.0, MeOH); ^{1}H NMR (400 MHz, CD_3OD) δ: 7.39–6.99 (m, 10H), 5.11 (br s, 1H), 4.57 (br s, 1H), 4.42 (t, *J* = 12.2 Hz, 1H), 4.28 (m, 1H), 4.11 (s, 1H), 3.14–2.89 (m, 8H), 2.86 (s, 3H), 2.78 (s, 3H), 2.68 (s, 1H), 2.56 (d, *J* = 5.0 Hz, 2H), 2.32 (s, 1H), 1.85–1.40 (m, 8H), 1.33–1.07 (m, 4H), 0.93 (m, 6H), −0.18 (br s, 1H); ^{13}C NMR (100 MHz, CD_3OD) δ: 175.5, 174.5, 174.3, 173.3, 171.9, 171.5, 170.6, 156.1, 155.7, 141.3, 139.5, 131.0 (×4), 130.1 (×4), 129.3 (×2), 63.3, 53.5, 53.2, 49.8, 48.5, 47.3 (×2), 42.0, 39.1, 34.9, 33.6, 32.6, 30.8, 29.9, 28.1, 26.6, 25.9, 25.8, 23.7, 23.1 (×2), 21.9; HR-MS (FAB, thioglycerol + glycerol, PEG600+NaI) calcd for $C_{44}H_{62}O_9N_{10}Na$: 897.4569 $[M+Na]^+$, found *m*/*z*: 897.4599 [M+Na].
24. Brurberg, M. B.; Eijsink, G. H.; Haandrikman, A. J.; Venema, G.; Nes, I. F. *Microbiology* **1995**, *141*, 123.
25. Hodge, A.; Gooday, G. W.; Alexander, J. *Phytochemistry* **1996**, *41*, 77.